Contents lists available at ScienceDirect

Arabian Journal of Chemistry

journal homepage: www.ksu.edu.sa

Design, synthesis and antifungal activity of indole derivatives containing 1,3,4-oxadiazole

Bangcan He, Yuzhi Hu, Piao Mao, Tianyu Deng, Yuhong Wang, Xingping Luo, Hongqian Zou, Zhenchao Wang *, Wei Xue *

National Key Laboratory of Green Pesticide, Key Laboratory of Green Pesticide and Agricultural Bioengineering, Ministry of Education, Center for R&D of Fine Chemicals of Guizhou University, Guiyang 550025, China

ARTICLE INFO

Keywords:
Indole
1,3,4-oxadiazole
Antifungal activity
Botrytis cinerea
Tomato Botrytis cinerea
Phomopsis sp

ABSTRACT

In this study, 21 indole derivatives containing 1,3,4-oxadiazole were designed and synthesized, the results of the biological activity test showed that the target compounds had certain antifungal activity against 12 plant pathogenic fungi *in vitro*, among which. **E1** showed excellent bioactivity against *Botrytis cinerea* (*B.c.*), *Tomato Botrytis cinerea* (*F.M.*) and *Phomopsis sp* (*P.s.*), with median effective concentration (EC_{50}) values of 2.8, 5.1 and 5.2 μg/mL, which are higher than those of the control drug azoxystrobin (Az) at 15.2, 31.2 and 15.2 μg/mL. *In vivo* tests on blueberry leaves, tomato leaves and kiwifruit showed that **E1** at 200 μg/mL offered stronger protective effect against *B.c.* (91.9 %) than Az (83.8 %) in blueberry leaves, *F.M.* (83.3 %) than Az (72.9 %) in tomato leaves and *P.s.* (89.3 %) than Az (86.9 %) in kiwifruit. Scanning electron microscope (SEM) experiments showed that *B.c.* hyphae treated with **E1** had abnormal shrinkage and obvious morphological changes. The results of the mechanism study showed that **E1** could change the integrity of the cell wall and cell membrane of pathogen *B.c.*, which led to the increase in malondialdehyde (MDA), cell leakage and permeability and the rupture of the cell membrane. Because of their strong antifungal effects on plant fungus, indole derivatives containing 1,3,4-oxadiazole were predicted to develop into novel fungicides.

1. Introduction

Plant fungal diseases were the main problem facing global agricultural production (Cui et al., 2020), which resulted in 10 % of post-harvest losses and a 20 % annual reduction in agricultural output. Furthermore, the mycotoxins produced by certain plant pathogenic fungi were dangerous to both human and animal health (Bräse et al., 2009). Plant pathogenic fungi such as *B.c.*, *F.M.* and *P.s.* had a substantial impact on agriculture (Gonzalez-Fernandez et al., 2011). reducing crop output and quality significantly. *B.c.* and *F.M.*, for example, can infect over 200 plants, including vegetables and minor fruit harvests (Ren et al., 2020). Plant pathogenic fungi are primarily accountable for fruit rot, leaf necrosis, and other diseases, collectively resulting in billions of dollars of annual losses globally (Ma et al., 2019; Tang et al., 2020). Fungicides were therefore crucial for maintaining production stability as well as increasing crop yield and quality (Liu et al., 2021). Furthermore, persistent fungicide usage has led to a number of drawbacks, including residual toxicity, drug resistance and environmental issues (Ren et al., 2020). Thus, in order to preserve plants, new environmental protection fungicides must be developed (Tleuova et al., 2020).

The design and development of molecules based on the structure of natural products is now one of the most active areas of drug research. Indole (Fig. 1) was an important natural substance that was a nitrogen-containing benzopyrrole alkaloid. Chimonanthus praecox's main skeleton was indole (Duan et al., 2023; Nunes, 2011). and its derivatives exhibit significant biological activity such as antifungal (Zheng et al., 2023), antibacterial (Silva et al., 2019; Tleuova et al., 2020), anticancer (Ribas e Ribas et al., 2016; Wang et al., 2022), antiviral (Seiber, 2011; Qian et al., 2010), excellent candidates for metal ion sensing (Alharthi, 2023) and so on. Indole derivatives were becoming a source of natural goods for health and environmental protection (Wu et al., 2007), which had become a hot issue in life science and chemistry as market demand grew.

One of the key five-membered nitrogen-containing heterocyclic compounds is 1,3,4-oxadiazole (Fig. 1), which has been studied

* Corresponding authors.
E-mail addresses: zcwang@gzu.edu.cn (Z. Wang), wxue@gzu.edu.cn (W. Xue).

https://doi.org/10.1016/j.arabjc.2024.105758
Received 17 January 2024; Accepted 24 March 2024
Available online 26 March 2024

Fig. 1. The structures of indole and 1,3,4-oxadiazole.

extensively in both medicine (Nowakowska, 2007) and organic synthesis (Chen et al., 2010). The 1,3,4-oxadiazole skeleton has been extensively studied and developed in the process of physiologically active recombination due to its incorporation of diverse functional building blocks (Tao et al., 2019; Fu et al., 2020). Fig. 2 depicts a commercial medicament that containing 1,3,4-oxadiazole. Furthermore, 1,3,4-oxadiazole compounds had anticancer (Du et al., 2013), antibacterial (Ouyang et al., 2021), antiviral (Jiang et al., 2020), antifungal (Zhu et al., 2016), insecticidal (Wang et al., 2019) and other biological properties.

To discover novel pesticide compounds exhibiting superior antifungal activities, we synthesized 21 indole derivatives incorporating the 1,3,4-oxadiazole moiety, leveraging the principle of active splicing in drug synthesis (Fig. 3 and Scheme 1). The *in vitro* antifungal activity of all the target compounds was tested against 12 plant pathogenic fungi using the mycelial growth rate method. The results of antifungal tests demonstrated that **E1** exhibited a pronounced inhibitory effect against *B.c.*, *F.M.* and *P.s.* Furthermore, *in vivo* experiments were conducted on blueberry leaves, tomato leaves and kiwifruit, utilizing compound **E1** at concentrations of 200 and 100 μg/mL. In order to further validate the antifungal activity of the studied series of compounds, SEM experiments and light microscope observation experiments showed that **E1** could alter the integrity of the cell wall and cell membrane of the pathogenic bacterium *B.c.*, leading to abnormal cell crumpling and leakage of contents, which led to an increase in the MDA, cellular leakage and cell permeability. This study identified indole derivatives exhibiting antifungal activities, establishing a theoretical foundation for the research, development and design of novel pesticides.

2. Materials and methods

2.1. Instruments and chemicals

2.1.1. Instruments

Experimental equipment utilized in this study is referenced from previously reported literature, providing a basis for equipment selection and experimental design (Zhou et al., 2023; Peng et al., 2022; Liu et al., 2023; Hu et al., 2023). Melting point measurements were performed by using the X-4B melting point instrument (Shanghai INESA Co., Ltd., Shanghai, China) without any modifications. The spectrum data were

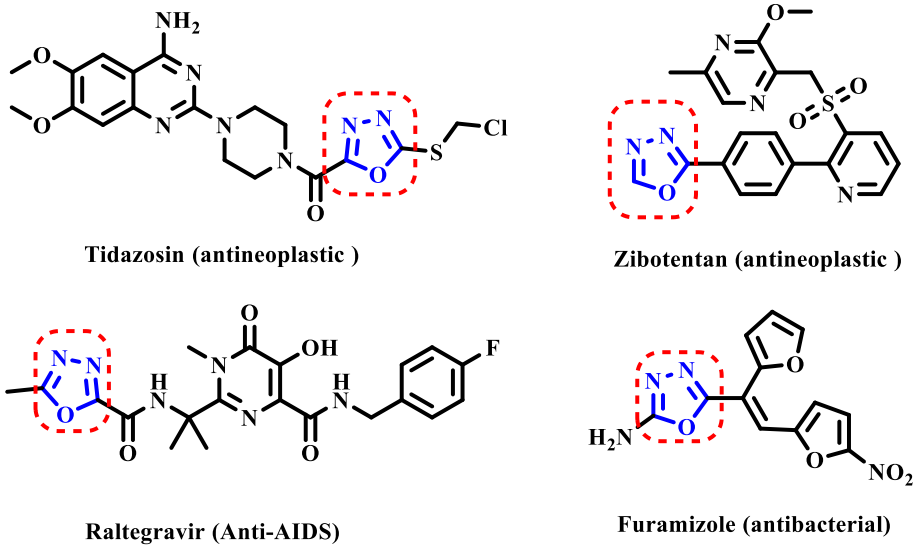

Fig. 2. Some commercial drugs contain 1,3,4-oxadiazole moiety.

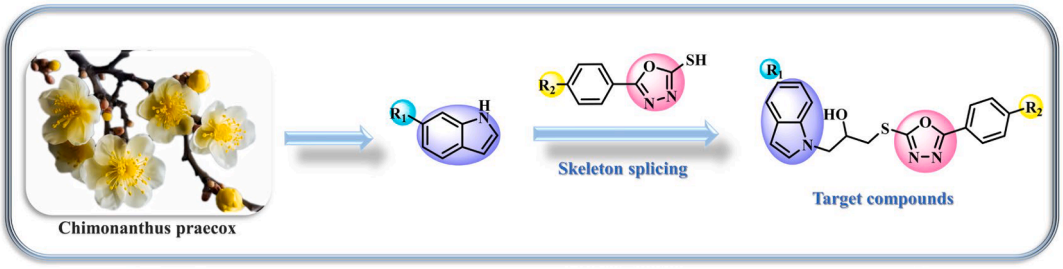

Fig. 3. Design of target compounds.

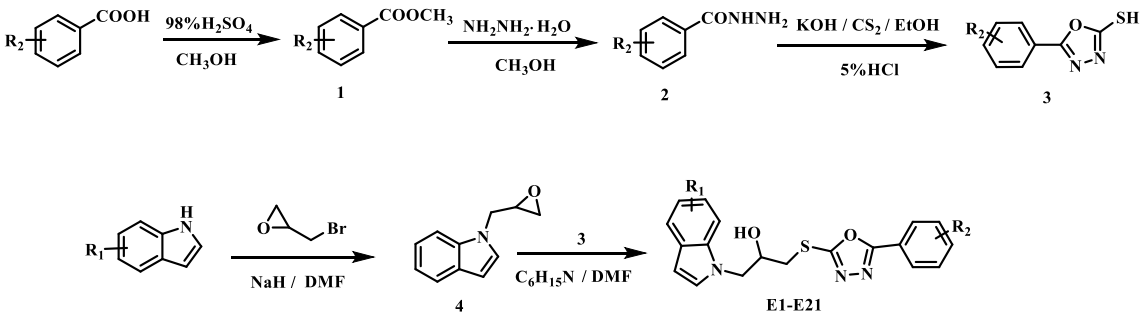

E1:R_1=H, R_2=4-CH_3
E2:R_1=H, R_2=H
E3:R_1=H, R_2=2-Cl
E4:R_1=H, R_2=3-Cl
E5:R_1=H, R_2=4-Cl
E6:R_1=H, R_2=2-Br
E7:R_1=H, R_2=4-F
E8:R_1=H, R_2=2,4-di-F
E9:R_1=5-Cl, R_2=2-Br
E10:R_1=5-Cl, R_2=4 -F
E11:R_1=5-Cl, R_2=4-CH_3
E12:R_1=5-Cl, R_2=2-OCH_3
E13:R_1=5-Br, R_2=2-Cl
E14:R_1=5-Br, R_2=4-F
E15:R_1=5-Br, R_2=4-Br
E16:R_1=5-Br, R_2=4-CH_3
E17:R_1=5-OCH_3 , R_2=2-Br
E18:R_1=5-OCH_3 , R_2=4-Br
E19:R_1=5-OCH_3 , R_2=4-Cl
E20:R_1=5-OCH_3 , R_2=4-CH_3
E21:R_1=5-OCH_3 , R_2=2,4-di-F

Scheme 1. Synthetic route of compounds **E1-E21**.

acquired by using a 500 NMR spectrometer (Bruker, Karlsruhe, Germany) and an ASCEND400 NMR spectrometer (Bruker, Germany). HRMS data were collected by using a hybrid quadrupole mass spectrometer from Thermo Scientific (Waltham, MA, USA). Cell permeability was measured by using the Leici DDSJ-3O8F conductivity meter (Shanghai Instrument & Electric Science Instrument Co., Ltd., China). Data for SEM were collected on an FEI Nova Nano 450 (Hillsboro, OR, USA). Cell leakage was detected by using the N-5000 UV spectrophotometer (Shanghai Yoke Instrument Co., Ltd., China). The microstructure was examined by using an optical microscope, specifically the Olympus CX21 model (Olympus, Japan).

2.1.2. Chemicals

Chemicals can be referenced based on previously reported literature (Ibrahim et al., 2017; Ibrahim et al., 2017; Li et al., 2017; Zhou et al., 2018; Meşeli et al., 2021; Peng et al., 2022). Reaction materials and chemicals, including carbon disulfide, epibromohydrin, substituted indole, various substituted benzoic acids, hydrazine hydrate and azoxystrobin (all A.R. grade) were obtained from Shanghai Titan Technology Co., Ltd., all analytical-grade reagents and solvents, including anhydrous ethanol, anhydrous methanol and *N*, *N*-dimethylformamide (DMF) were commercially obtained. Additional chemical materials were sourced from Bositai Technology Co., Ltd. (Chongqing, China).

2.2. Synthesis

2.2.1. Synthesis of intermediates *1–4*

Intermediates **1**–**4** were synthesized using slightly modified procedures reported in the literature (Peng et al., 2021; Ibrahim et al., 2017; Li et al., 2017; Zhou et al., 2018; Meşeli et al., 2021). (Using **E2** as an illustrative example, intermediates **1**–**4** are methyl benzoate, benzohydrazide, 5-phenyl-1,3,4-oxadiazole-2-thiol and 1-(oxiran-2-ylmethyl)-1*H*-indole, respectively). Different substitutes for benzoic acid were used in acidic conditions, such as methanol as a solvent in an esterification reaction that took 7 h to produce intermediate **1**, methanol as a solvent in a reaction that took 7 h to produce intermediate **2**, ethanol as a solvent in an alkaline condition that took 8 h to produce carbon disulfide (CS_2), and finally 5 % HCl acidification to produce intermediate **3**. In the replacement of indole as a raw material in the strong alkaline conditions of NaH and bromopropylene oxide at 45 °C at a temperature of heating and reflux for 6 h to produce intermediate **4**.

2.2.2. Synthesis of target compounds *E1-E21*

Dissopropylamine (8.66 mmol) and 20 mL of DMF were added to a round-bottom flask along with Intermediate **4** (2.89 mmol). Intermediate **3** (3.18 mmol) was added to the reaction mixture after 30 min. TLC was used to track the reaction's course for around 10 h at 77 °C. TLC was used to carry out the reaction. The reaction was heated, then combined with 90 mL of distilled water and extracted with ethyl acetate. The upper liquid phase was recovered, dried, filtered and the ethyl acetate solvent was removed after three washes with saturated brine. Finally, **E1-E21** were purified by column chromatography (petroleum ether: ethyl acetate = 10:1, *v/v*) (Ibrahim et al., 2017). The synthetic route of **E1-E21** was shown in Scheme 1**.** The **Supporting Information** contains detailed characterization data for **E1-E21**.

2.3. Antifungal bioassays

2.3.1. In vitro antifungal activity assay

According to the mycelium growth rate approach mentioned in references (Jang et al., 2012; Wan et al., 2015; Ibrahim et al., 2017). Dimethylsulfoxide (DMSO) was utilized as a blank control, whereas Az served as the positive control. At a concentration of 100 μg/mL, the antifungal activity of **E1-E21** against 12 types of *B.c.*, *Rhizoctonia solani* (*R.s.*), *Phytophthora capsica* (*P.c.*), *Sclerotinia sclerotiorum* (*S.s.*), *F.M.*, *P.s.*, *Neoscytalidium dimidiatum (N.d.*), *Colletotrichum gloeosporioides* (*C.g.*), *pepper anthracnose* (*P.a.*), *Botryosphaeria dothidea* (*B.d.*), *Fusarium graminearum* (*F.g.*) and *Fusarium asiaticum* (*F.a.*) were determined *in vitro*. Concurrently, the EC_{50} values for compounds exhibiting strong antifungal properties were determined, with the experimental protocol outlined in the **Supporting Information**.

2.3.2. In vivo antifungal activity assay

The experiment was carried out in accordance with the procedure described in the literature (Zhou et al., 2015; Wang et al., 2023; Zhou et al., 2023). By using DMSO as a blank control and Az as positive

Table 1
In vitro antifungal activity of **E1-E21** at 100 μg/mL [a].

Compd.	Inhibition rate (%)											
	B.c.[b]	*R.s.*	*P.c.*	*S.s.*	*F.M.*	*P.s.*	*N.d.*	*C.g.*	*P.a.*	*B.d.*	*F.g.*	*F.a.*
E1	100	41.4 ± 1.5	36.5 ± 1.1	53.7 ± 1.4	80.5 ± 1.6	89.6 ± 1.7	35.8 ± 0.9	72.7 ± 0.0	71.6 ± 0.0	45.1 ± 1.5	51.0 ± 1.6	49.4 ± 0.9
E2	99.6 ± 0.9	53.7 ± 1.6	49.2 ± 1.1	78.0 ± 1.4	69.3 ± 0.9	85.4 ± 1.7	46.4 ± 1.4	67.4 ± 2.6	64.7 ± 2.4	47.7 ± 1.3	43.6 ± 1.7	50.2 ± 0.9
E3	94.6 ± 1.7	55.6 ± 1.5	48.4 ± 1.1	76.8 ± 1.2	77.3 ± 1.8	87.1 ± 0.9	54.2 ± 0.7	69.4 ± 1.1	69.0 ± 1.4	35.2 ± 1.7	56.0 ± 1.9	56.9 ± 0.9
E4	84.0 ± 0.9	70.9 ± 1.8	38.1 ± 0.0	60.6 ± 1.6	64.1 ± 1.4	74.2 ± 1.1	38.8 ± 0.9	55.0 ± 0.9	52.6 ± 2.4	15.2 ± 1.1	34.7 ± 1.6	39.3 ± 1.7
E5	77.4 ± 1.7	67.5 ± 1.1	37.3 ± 1.1	58.9 ± 0.9	64.9 ± 1.1	82.1 ± 1.7	80.9 ± 1.7	35.1 ± 0.9	59.5 ± 1.9	50.8 ± 2.8	51.7 ± 1.6	51.9 ± 1.7
E6	100	73.9 ± 1.0	36.9 ± 1.2	62.6 ± 1.8	56.6 ± 0.9	87.5 ± 1.4	62.4 ± 0.9	32.6 ± 0.9	62.5 ± 1.3	43.2 ± 1.3	61.8 ± 1.7	50.6 ± 1.2
E7	90.7 ± 0.0	71.3 ± 0.8	33.7 ± 1.6	62.6 ± 1.8	75.3 ± 1.7	67.9 ± 1.7	83.0 ± 0.9	45.0 ± 0.9	61.2 ± 1.4	26.1 ± 1.7	43.6 ± 1.7	48.5 ± 2.3
E8	75.5 ± 1.1	65.7 ± 1.0	42.9 ± 2.3	59.8 ± 1.8	61.8 ± 1.4	78.8 ± 1.2	55.5 ± 1.4	38.4 ± 0.9	54.3 ± 1.2	24.6 ± 0.8	47.5 ± 1.1	42.7 ± 0.9
E9	100	66.4 ± 0.0	38.1 ± 0.0	46.7 ± 0.9	65.3 ± 1.8	74.6 ± 1.7	77.3 ± 0.9	34.7 ± 1.1	55.2 ± 2.4	18.9 ± 1.1	52.1 ± 1.1	45.2 ± 0.9
E10	94.2 ± 1.7	75.7 ± 1.5	47.6 ± 1.3	61.8 ± 1.1	68.1 ± 1.1	74.2 ± 1.8	64.8 ± 0.9	34.3 ± 1.2	57.8 ± 1.2	43.2 ± 1.3	52.1 ± 1.1	45.2 ± 0.9
E11	94.9 ± 0.9	73.1 ± 1.3	49.2 ± 1.1	57.3 ± 1.2	75.7 ± 0.9	69.2 ± 1.1	61.8 ± 1.1	43.4 ± 0.9	53.4 ± 1.4	48.5 ± 1.1	47.9 ± 1.1	49.0 ± 1.2
E12	96.9 ± 2.2	71.3 ± 0.8	44.8 ± 0.9	54.9 ± 1.2	55.4 ± 1.1	72.9 ± 0.9	58.2 ± 1.1	31.4 ± 1.1	51.3 ± 0.9	43.9 ± 1.1	57.5 ± 1.1	41.4 ± 1.2
E13	97.3 ± 1.6	67.5 ± 1.1	39.7 ± 1.1	46.7 ± 1.6	64.9 ± 1.7	70.4 ± 0.9	86.1 ± 0.9	45.9 ± 0.9	52.6 ± 1.2	52.3 ± 1.3	45.6 ± 1.1	36.0 ± 1.2
E14	98.8 ± 1.1	78.0 ± 0.8	33.7 ± 0.9	70.3 ± 0.9	74.5 ± 1.7	75.4 ± 0.9	66.7 ± 0.9	35.5 ± 1.4	52.2 ± 1.3	68.9 ± 1.7	57.5 ± 1.1	51.5 ± 1.2
E15	98.8 ± 1.1	67.5 ± 1.1	46.0 ± 1.1	61.0 ± 1.4	75.3 ± 1.7	74.2 ± 1.8	60.6 ± 0.9	37.6 ± 0.9	49.1 ± 1.2	37.5 ± 1.1	48.6 ± 0.8	46.4 ± 1.2
E16	98.8 ± 1.1	78.4 ± 1.0	48.4 ± 1.1	70.3 ± 1.6	75.3 ± 1.1	84.6 ± 0.9	86.1 ± 0.9	40.9 ± 0.9	68.1 ± 1.2	45.1 ± 1.5	47.1 ± 0.8	46.9 ± 1.7
E17	75.5 ± 1.1	64.9 ± 1.6	31.3 ± 0.9	54.1 ± 0.9	73.7 ± 1.4	72.1 ± 2.2	74.2 ± 1.3	44.2 ± 1.2	57.8 ± 2.4	20.8 ± 0.8	37.1 ± 1.6	40.2 ± 0.9
E18	90.3 ± 0.9	71.3 ± 0.8	39.7 ± 1.1	54.1 ± 0.9	72.5 ± 2.9	82.9 ± 0.9	53.9 ± 0.9	27.7 ± 1.7	62.5 ± 1.9	38.6 ± 1.3	59.5 ± 1.1	39.3 ± 2.2
E19	74.7 ± 0.9	70.1 ± 1.0	31.7 ± 1.1	46.7 ± 0.9	74.1 ± 2.1	73.3 ± 1.1	51.8 ± 0.9	33.5 ± 0.9	52.6 ± 1.2	33.7 ± 1.5	53.7 ± 1.3	42.7 ± 0.9
E20	63.4 ± 1.1	64.6 ± 0.8	36.5 ± 1.1	47.6 ± 1.2	71.7 ± 0.9	79.6 ± 0.9	66.4 ± 0.9	47.1 ± 1.1	53.0 ± 0.9	19.3 ± 1.7	58.3 ± 1.3	40.2 ± 0.9
E21	91.8 ± 1.1	59.0 ± 1.0	38.1 ± 1.3	46.3 ± 1.4	62.9 ± 1.8	78.8 ± 1.9	67.0 ± 0.7	31.8 ± 1.2	61.2 ± 0.0	10.2 ± 1.1	46.3 ± 1.6	33.5 ± 1.2
Az[c]	72.4 ± 0.9	86.6 ± 1.3	61.1 ± 1.7	75.6 ± 0.0	66.1 ± 0.9	66.7 ± 1.1	72.4 ± 0.7	62.4 ± 1.7	68.5 ± 1.7	72.0 ± 2.1	57.9 ± 0.8	66.5 ± 1.8

[a] Values are mean ± SD of three replicates. [b] *Botrytis cinerea* (*B.c.*), *Rhizoctonia solani* (*R.s.*), *Phytophthora capsica* (*P.c.*), *Sclerotinia sclerotiorum* (*S.s.*), *Tomato Botrytis cinerea* (*F.M.*), *Phomopsis sp* (*P.s.*), *Neoscytalidium dimidiatum (N.d.*), *Colletotrichum gloeosporioides* (*C.g.*), *pepper anthracnose* (*P.a.*), *Botryosphaeria dothidea* (*B.d.*), *Fusarium graminearum* (*F.g.*), *Fusarium asiaticum* (*F.a.*). [c]Commercial antifungal agent azoxystrobin (Az) were used as the control agents.

Table 2
The EC_{50} values of several target compounds [a].

Comp.	Pathogens	Regression equation	Correlation coefficient (r)	EC_{50} (μg/mL)
E1	*B.c.*	y = 1.2820x + 4.4289	0.9805	2.8
E2	*B.c.*	y = 1.3824x + 4.2676	0.9865	3.4
E3	*B.c.*	y = 1.4319x + 3.6964	0.9834	8.1
E6	*B.c.*	y = 1.1322x + 3.9748	0.9966	8.0
E7	*B.c.*	y = 1.2106x + 4.0952	0.9736	5.6
E9	*B.c.*	y = 1.0571x + 4.3265	0.9390	4.3
E16	*B.c.*	y = 1.3392x + 3.9345	0.9874	6.2
E21	*B.c.*	y = 0.9753x + 4.0997	0.9792	8.4
Az[b]	*B.c.*	y = 1.2756x + 3.4941	0.9719	15.2
E1	*F.M.*	y = 0.7209x + 4.4875	0.9914	5.1
E2	*F.M.*	y = 0.8248x + 4.1566	0.9947	10.5
E3	*F.M.*	y = 0.7323x + 4.4745	0.9546	5.2
E14	*F.M.*	y = 0.8012x + 4.0792	0.9882	14.1
E16	*F.M.*	y = 1.0992x + 3.7151	0.9879	14.8
Az[b]	*F.M.*	y = 0.8368x + 3.7501	0.9882	31.2
E1	*P.s.*	y = 0.9305x + 4.3315	0.9701	5.2
E2	*P.s.*	y = 1.1486x + 4.0831	0.9671	6.3
E3	*P.s.*	y = 1.2638x + 3.8911	0.9878	7.5
E5	*P.s.*	y = 1.1266x + 3.9234	0.9859	9.0
E6	*P.s.*	y = 0.9664x + 4.2582	0.9985	5.9
E8	*P.s.*	y = 0.7920x + 4.3938	0.9252	5.8
E16	*P.s.*	y = 1.1072x + 3.9203	0.9845	9.4
E18	*P.s.*	y = 0.8859x + 4.3441	0.9792	5.5
E20	*P.s.*	y = 0.9939x + 4.1062	0.9805	7.9
E21	*P.s.*	y = 1.0582x + 4.0994	0.9770	7.1
Az[b]	*P.s.*	y = 1.2756x + 3.4941	0.9719	15.2
E1	*S.s.*	y = 0.6179x + 4.2931	0.9924	13.9
E2	*S.s.*	y = 1.0074x + 3.8229	0.9973	14.7
E3	*S.s.*	y = 0.8141x + 4.2253	0.9735	8.9
Az[b]	*S.s.*	y = 0.8912x + 3.8616	0.9860	18.9

[a] Average of three replicates. [b] The Commercial antifungal agents.

control, the curative and protective activities of **E1** with the greatest antifungal activity on blueberry leaves, tomato leaves and kiwifruit *in vivo* were evaluated. The experimental method was provided in the **Supporting Information**.

2.3.3. Scanning electron microscopy (SEM) characterization

The approach described in the literature was used to conduct the SEM experiment (Su et al., 2021; Zhang et al., 2018). *B.c.* mycelium was treated with various doses of **E1**. The experimental approach was described in the **Supporting Information**.

2.3.4. Cytoplasmic leakage volume assay

To investigate other possible action modes of **E1** on *B.c.* mycelium, the absorbance of the supernatant of *B.c.* mycelium treated with **E1** was measured by using an ultraviolet spectrophotometer at 260 and 280 nm, as described in the literature (Liu et al., 2023; Ma et al., 2019). Secondly, the MDA content of **E1** was measured to indirectly reflect the degree of tissue peroxidation damage to the mycelium membrane (Chen et al., 2023; Zhou et al., 2023). In this investigation, two distinct approaches were utilized to investigate the degree of **E1** damage to *B.c.* mycelium, which resulted in cytoplasmic leakage. Experimental methods were provided in the **Supporting Information**.

2.3.5. Optical microscope characterization

By using an optical microscope, the effect of the most active **E1** on *B.c.* mycelium was observed according to the method reported in the literature (Liu et al., 2023).

2.3.6. Characteristics of cell membrane permeability

The effect of **E1** on cell permeability was assessed with the method described in the literature (Efenberger-Szmechtyk et al., 2021; Shang et al., 2019; Zhou et al., 2023), and the relative conductivity of mycelium suspensions containing varying doses of **E1** was determined at various times. The experimental approach was described in the **Supporting Information**.

3. Results and discussion

3.1. Chemistry

Following the synthetic route outlined in Scheme 1, a series of indole derivatives (**E1-E21**) incorporating the 1,3,4-oxadiazole moiety were synthesized. The structure of the target compounds was preliminary characterized by NMR and HRMS, and detailed data were provided in the **Supporting Information**.

3.2. In vitro antifungal activity analysis

The inhibitory activity of the target compounds against 12 distinct plant pathogenic fungi was assessed at a concentration of 100 μg/mL using mycelium growth inhibition assay, with Az serving as the control agent for comparison. Table 1 shows all 21 indole derivatives with the 1,3,4-oxadiazole moiety inhibited *B.c.* by 74.7–100.0 %, outperforming the commercial Az (72.4 %). **E1**, **E6** and **E9** exhibited 100 % inhibition against *B.c.*, demonstrating strong anti-*B.c.* activity. **E2** (78.0 %) and **E3** (76.8 %) showed better inhibition of *S.s.* than Az (75.6 %), with minimal impact overall. Simultaneously, it exerts an inhibitory effect on *F.M.* Specifically, the inhibitory range of **E1**, **E2**, **E3**, **E7**, **E10**, **E11**, **E14**, **E15**, **E16**, **E17**, **E18**, **E19** and **E20** was 68.1–80.5 %, exceeding the inhibitory effect of the control drug Az, which was 66.1 %. All 21 compounds synthesized concurrently demonstrated good inhibitory activity against *P.s.*, with an inhibitory range of 67.9–89.6 %, outperforming the control drug Az (66.7 %). Among these compounds, **E5** (80.9 %), **E7** (83.0 %), **E9** (77.3 %), **E13** (86.1 %), **E16** (86.1 %) and **E17** (74.2 %) demonstrated superior inhibitory effects against *N.d.* compared to the control medication Az (72.4 %). They exhibit certain inhibitory effects against *C.g.*, with **E1** (72.7 %), **E2** (67.4 %) and **E3** (69.4 %) demonstrating stronger inhibitory actions compared to Az (62.4 %). **E1** (71.6 %) and **E3** (69.0 %) demonstrated stronger inhibitory effects on *P.a.* compared to Az (68.5 %). Similarly, **E6** (61.8 %) displayed higher inhibitory activity against *F.g.* than Az (57.9 %). To verify the antifungal activity of these compounds, we determined the EC_{50} values of the compounds exhibiting stronger inhibitory activity than the control agent at a concentration of 100 μg/mL. The results are presented in Table 2 and Fig. 4. The EC_{50} values of **E1**, **E2**, **E3**, **E6**, **E7**, **E9**, **E16** and **E21** against *B.c.* were 2.8, 3.4,

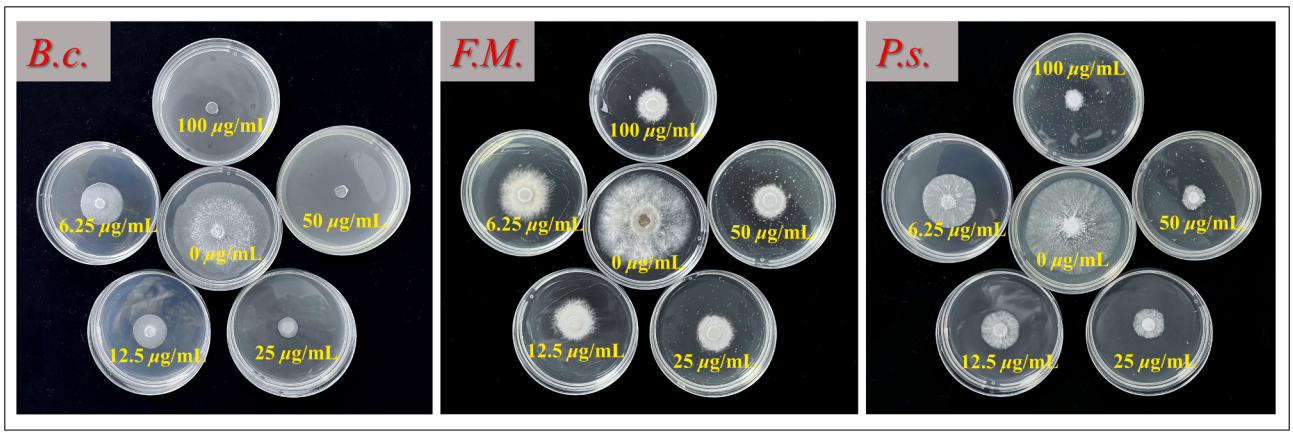

Fig. 4. The EC_{50} figure of antifungal activities of **E1** against *Botrytis cinerea* (*B.c.*), *Tomato Botrytis cinerea* (*F.M.*) and *Phomopsis sp* (*P.s.*).

Table 3
In vivo control effects of **E1** against *Botrytis cinerea.*

Compound	Concentration (μg/mL)	Curative effect		Protective effect	
		Lesion length [a] (mm ± SD)	controlling efficacy (%)	Lesion length [a] (mm ± SD)	Controlling efficacy (%)
E1	200	7.2 ± 0.4	86.3 ± 1.9	6.3 ± 0.7	91.9 ± 3.8
	100	12.7 ± 0.5	51.6 ± 2.4	9.0 ± 0.6	75.8 ± 2.9
Az [b]	200	12.0 ± 0.6	55.8 ± 2.9	7.7 ± 0.5	83.8 ± 2.4
	100	17.0 ± 0.8	24.2 ± 4.2	12.2 ± 0.9	56.6 ± 4.6
control	–	20.8 ± 0.7	–	21.5 ± 0.5	–

[a] Values are mean ± SD of three replicates. [b] The Commercial antifungal agents.

8.1, 8.0, 5.6, 4.3, 6.2 and 8.4 μg/mL, respectively, these values were superior to that of Az (15.2 μg/mL), and with **E1** performing best with an EC_{50} of 2.8 μg/mL. In addition, **E1**, **E2**, **E3**, **E14** and **E16** exhibited EC_{50} values of 5.1, 10.5, 5.2, 14.1 and 14.8 μg/mL against *F.M.*, outperforming Az (31.2 μg/mL). Meanwhile, **E1**, **E2**, **E3**, **E5**, **E6**, **E8**, **E16**, **E18**, **E20** and **E21** showed EC_{50} values of 5.2, 6.3, 7.5, 9.0, 5.9, 5.8, 9.4, 5.5, 7.9 and 7.1 μg/mL against *P.s.*, which was superior to that of Az (15.2 μg/mL). And lastly **E1**, **E2** and **E3** showed EC_{50} values of 13.9, 14.7 and 8.9 μg/mL against *S.s.*, which was better than that of Az (18.9 μg/mL). Based on these results, **E1** demonstrates potent broad-spectrum antifungal activity. In summary, the incorporation of 1,3,4-oxadiazole-containing indole derivatives into the structure enhances antifungal activity.

3.3. Structure-activity relationship of antifungal activity

Utilizing the data presented in Table 1 along with the structure of the target compounds, a detailed structure–activity relationship analysis was conducted, revealing that the introduction of 1,3,4-oxadiazole into the indole moiety significantly enhances antifungal activity. This series of compounds demonstrated remarkable antifungal activity against *B.c.* Introducing either electron-withdrawing or electron-donating groups further enhances their antifungal activity. Specifically, the presence of the 1,3,4-oxadiazole moiety effectively boosts antifungal activity. In relation to other examined fungi, compounds with R_1 = H exhibited stronger inhibitory effects than those with R_1= (Br, Cl). This was evident in the anti-*S.s.* activity of **E2** and **E3**, the anti-*F.M.* activity of **E1**, **E2**, **E3** and **E7**, as well as the inhibitory activities against *P.s.* (**E1**, **E2**, **E3**, **E5** **E6**), *C.g.* (**E1**, **E2**, **E3**) and *P.a.* (**E1**, **E2**). Furthermore, when R_2 = 4-CH_3-Ph, H, 2-Cl-Ph, 3-Cl-Ph, 4-Cl-Ph, 2-Br-Ph and 4-F-Ph, it inhibits several fungi. Moreover, the compound's antifungal activity test suggests that the indole ring R_1 can exhibit strong antifungal activity in the presence of electron-donating substituents. Regardless of whether R_2 features electron-donating or electron-withdrawing substituents, the antifungal activity of this series of compounds can be enhanced. Specifically, **E1** (R_1 = H, R_2 = CH_3) exhibited remarkable antifungal activity against multiple fungal species. As a result of the aforementioned analysis, the highly bioactive representative **E1** was selected for subsequent *in vivo* and mechanistic investigations.

3.4. Bioactivity test results of *E1* against B.c., f.m. And p.s. In vivo

The *in vitro* and EC_{50} experimental results demonstrated that **E1** exhibited excellent antifungal activity against three plant pathogens: *B.c.*, *F.M.* and *P.s.* To further investigate the inhibitory effect of **E1** in a real-world setting, fresh, uniformly sized and undamaged blueberry leaves, tomato leaves and kiwifruit fruits were chosen for experimental evaluation, using agricultural fungicide Az as a control. **E1** showed superior fungicidal activity against *B.c.* compared to the control. Its *in vivo* performance on blueberry leaves with EC_{50} = 2.8 μg/mL was tested and results are in Table 3 and Fig. 5. Firstly, **E1** exhibited protective activities of 91.9 % and 75.8 % at 200 and 100 μg/mL, outperforming Az with 83.8 % and 56.6 %, respectively. Its curative efficacies were 86.3 % and 51.6 % at the same concentrations, surpassing Az's 55.8 % and 24.2 %.

Secondly, **E1** with excellent anti-*F.M.* activity (EC_{50} = 5.1 μg/mL) in tomato leaves was studied *in vivo*, as shown in Table 4 and Fig. 6. The protective activity of **E1** was 83.3 and 71.9 % at 200 and 100 μg/mL, respectively, which was superior to that of Az (72.9 and 55.2 %, respectively). In terms of curative efficacy, **E1** demonstrated an equivalent performance of 79.2 % at 200 μg/mL compared to Az's 80.2 %. Notably, **E1**'s effective rate of 62.3 % at 100 μg/mL surpassed Az's rate of 37.7 %. At the same time, kiwifruit was a favorite fruit for people, but fungal infection will greatly reduce the yield and death of fruit trees, so it was more significant to study drugs with resistance to *P.s.* Therefore, the current study aimed to further investigate **E1** excellent anti-*P.s.* activity (EC_{50} = 5.2 μg/mL) through *in vivo* experiments. As presented in Table 5 and Fig. 7. The protective activity of **E1** was 89.3 % and 79.4 % at concentrations of 200 and 100 μg/mL, respectively, exceeding the

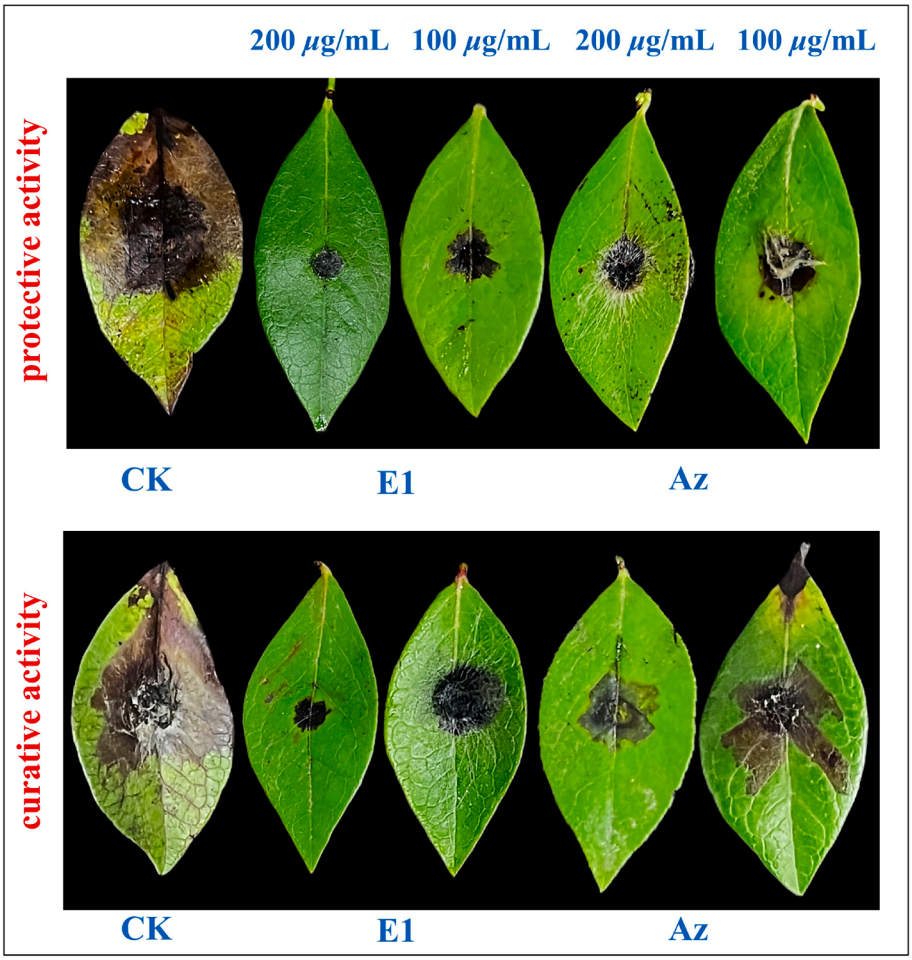

Fig. 5. *In vivo* control effects of **E1** against *Botrytis cinerea* (*B.c.*) on blueberry leaves.

Table 4
In vivo control effects of **E1** against *Tomato Botrytis cinerea.*

Compound	Concentration (μg/mL)	Curative effect		Protective effect	
		Lesion length [a] (mm ± SD)	controlling efficacy (%)	Lesion length [a] (mm ± SD)	controlling efficacy (%)
E1	200	8.7 ± 0.5	79.2 ± 2.5	7.7 ± 0.5	83.3 ± 2.5
	100	11.7 ± 0.7	62.3 ± 3.9	9.5 ± 0.8	71.9 ± 4.0
Az [b]	200	8.5 ± 0.8	80.2 ± 4.0	9.3 ± 0.9	72.9 ± 4.9
	100	16.0 ± 0.6	37.7 ± 3.0	12.2 ± 0.4	55.2 ± 1.9
control	–	22.7 ± 0.5	–	21.0 ± 0.8	–

[a] Values are mean ± SD of three replicates. [b] The Commercial antifungal agents.

corresponding values for Az, which were 86.9 % and 69.6 %. Similarly, the curative efficacy of **E1** at the same concentrations was 85.7 % and 68.8 %, respectively, outperforming Az's curative efficacy of 77.7 % and 66.5 %. Thus, we can conclude that **E1** had better curative and protective activity than Az *in vivo*, which was consistent with the crude screening and EC_{50} results. It was further confirmed that the inhibition was better when R_2 was an electron-giving group such as -CH_3. These intriguing findings imply that the integration of 1,3,4-oxadiazole into indoles holds promise as a potential agricultural fungicide for the management of fungal diseases.

3.5. *Observation results of mycelium morphology by **E1** scanning electron microscope (SEM)*

The mycelium of *B.c.* was further analyzed by using SEM, with the findings presented in Fig. 8. Notably, the morphology of the mycelium treated with **E1** exhibited substantial alterations. In contrast, the untreated group exhibited an intact and robust mycelium. However, when the concentration of **E1** was 50 μg/mL, the mycelia appeared curled and wrinkled and the surface was uneven. When the drug concentration increased to 100 μg/mL, the mycelium wrinkled more obviously, shrunk, the mycelium content leaked and the mycelium ruptured. Therefore, it was concluded that the inhibitory effect of **E1** on *B.c.* was achieved by altering the integrity of the cell wall and cell membrane of *B.c.*, disrupting its mycelial morphology and affecting mycelial growth. The reason for the 100 % inhibition of *B.c.* by **E1** in the *in vitro* inhibition test results at a concentration of 100 μg/mL was further verified.

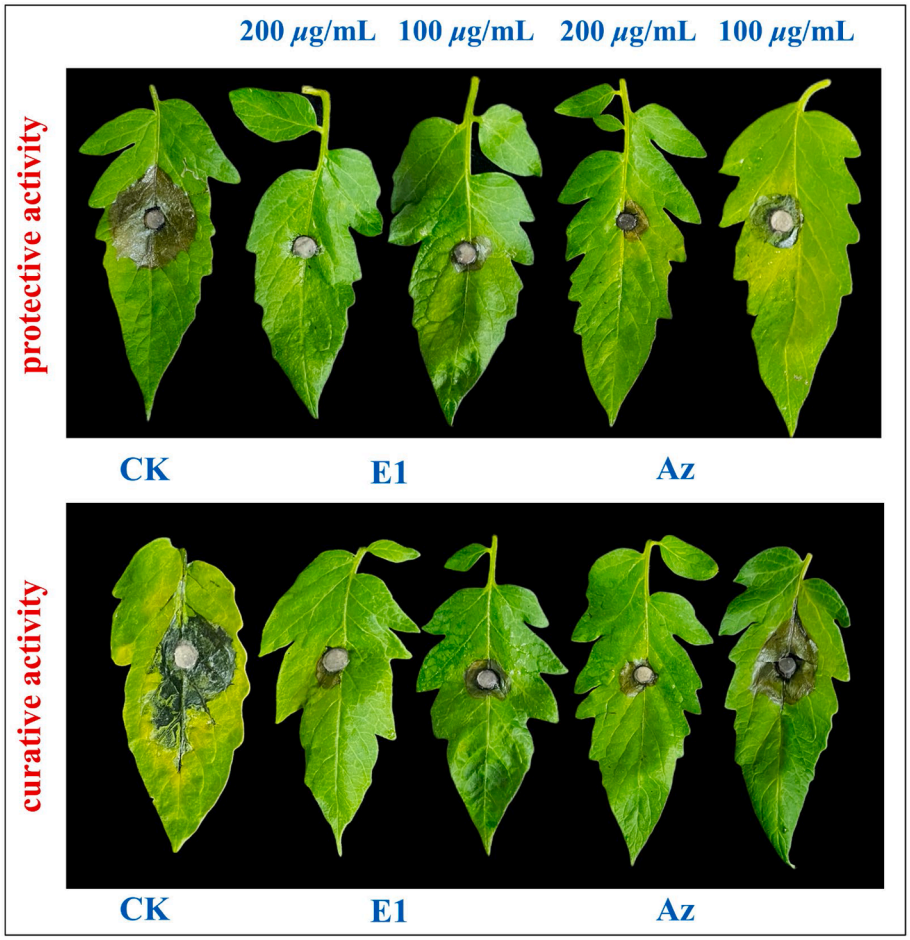

Fig. 6. *In vivo* control effects of **E1** against *Tomato Botrytis cinerea* (*F.M.*) on tomato leaves.

Table 5
In vivo control effects of **E1** against *Phomopsis sp.*

Compound	Concentration (μg/mL)	Curative effect		Protective effect	
		Lesion length [a](mm ± SD)	Controlling fficacy (%)	Lesion length [a] (mm ± SD)	Controlling efficacy (%)
E1	200	10.3 ± 0.7	85.7 ± 2.0	8.8 ± 0.7	89.3 ± 1.9
	100	16.7 ± 0.5	68.8 ± 1.3	12.3 ± 0.5	79.4 ± 1.3
Az [b]	200	13.3 ± 0.9	77.7 ± 2.5	9.7 ± 0.7	86.9 ± 2.0
	100	17.5 ± 0.8	66.5 ± 2.1	15.8 ± 0.4	69.6 ± 1.0
control	–	42.3 ± 0.5	–	40.7 ± 0.9	–

[a] Values are mean ± SD of three replicates. [b] The Commercial antifungal agents.

3.6. *The implications of **E1** on the cytoplasmic leakage of b.c.*

In order to investigate other potential mechanisms of action of **E1**, the current study employed two different methods to assess the degree of mycelial damage subsequent to the compound's activity, which results in the leakage of cytoplasmic contents. The results were displayed in Fig. 9. In particular, the absorbance of the mycelial supernatant of blueberry gray mold treated with **E1** at 260 and 280 nm was measured using a UV spectrophotometer. Furthermore, during the course of 10 h, the absorbance of the mycelial supernatant of the mycelium treated with **E1** at 260 and 280 nm was proportionate to the concentration. Second, the concentration of MDA can serve as an indirect indicator of the extent of tissue peroxidative damage to the mycelial membrane, the higher the content, the more severe the damage to the cell membrane. When the concentration of **E1** (0, 25, 50, 100 and 200 μg/mL) was applied to *B.c.* mycelium, the MDA content grew progressively. These concentrations were all better than what the control group had. The results showed that **E1** causes damage to cell membranes, with the degree of damage increasing with concentration. The degree of cytoplasmic content leakage rose, which shows that **E1** may also destroy the structure of the cell membrane by destroying the permeability of the cell membrane, so that drugs can penetrate bacteria and combine with some enzymes, affecting the activity of enzymes and thus achieving an antifungal effect.

3.7. ***E1** observation through the light microscope on the hyphae morphology*

After treatment with **E1** (25 μg/mL), the mycelium of *B.c.* was observed under an optical microscope (A, C) (10/1.25) and (B, D) (40/0.65), as shown in Fig. 10. Specifically, in the blank control group (A, B) (0.5 % DMSO) without drug treatment, the mycelium surface was smooth and had few branches. However, after **E1** (C, D) treatment, it was observed that the mycelium branches increased, the mycelium was disorderly and staggered and the mycelium thickness distribution was

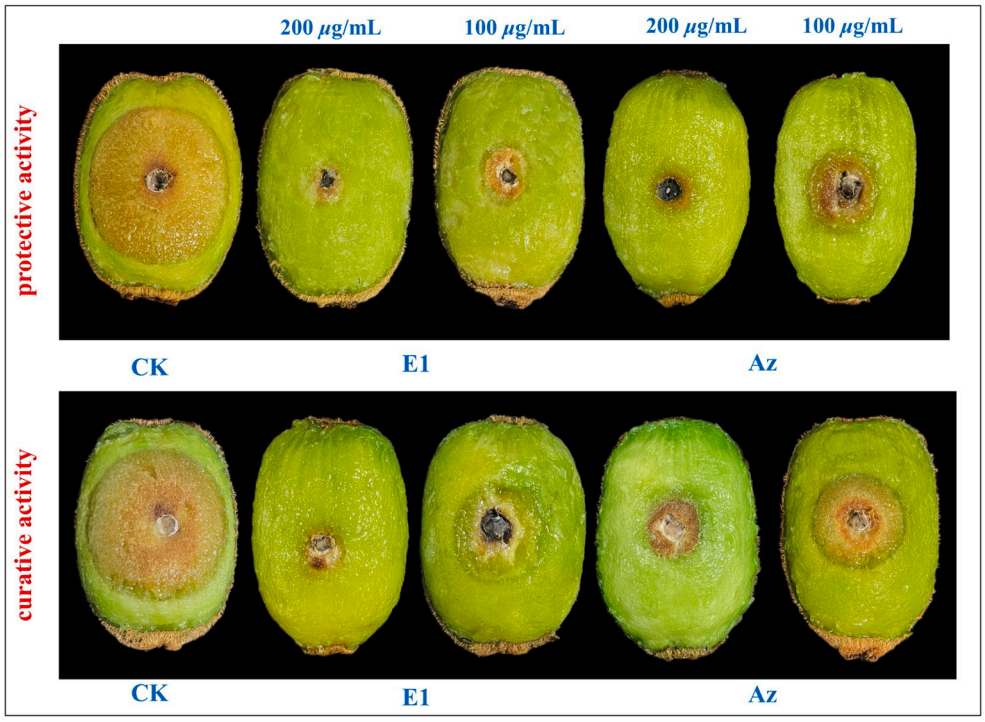

Fig. 7. *In vivo* control effects of **E1** against *Phomopsis sp* (*P.s.*) on kiwifruit.

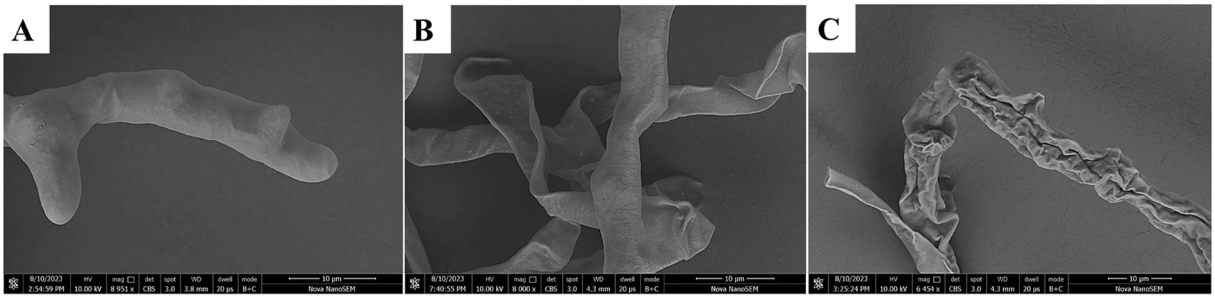

Fig. 8. SEM images of the hyphae of *Botrytis cinerea* (*B.c.*) after treatment with **E1**. (A) 0 μg/mL, (B) 50 μg/mL and (C) 100 μg/mL. Scale bar for (A-C) are 20 μm.

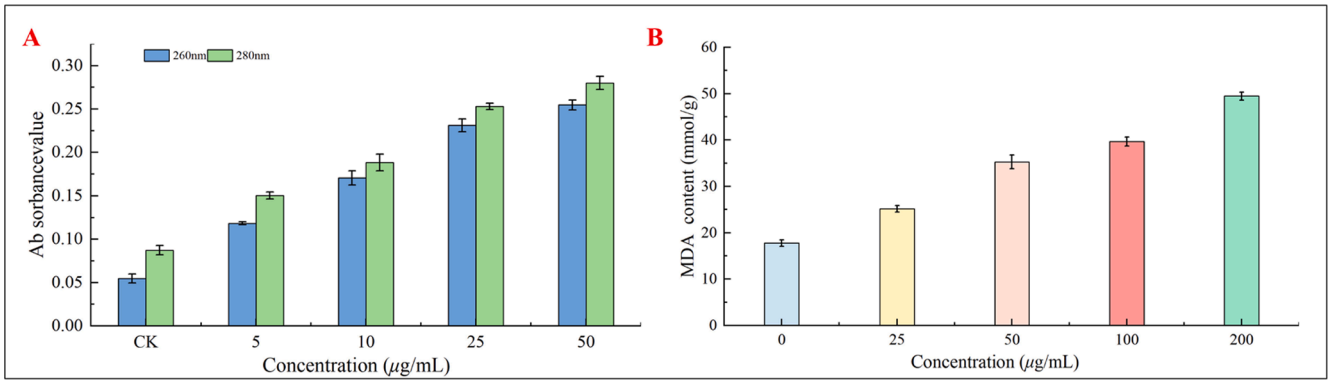

Fig. 9. Leakage of cytoplasmic contents after **E1** action on *Botrytis cinerea* (*B.c.*) hyphae was determined by UV spectrophotometry (A) and MDA (B).

uneven. It can be proven that the compound had a good inhibitory effect on the growth of fungi. This further explains why **E1** was able to inhibit mycelial growth with excellent inhibitory activity against *B.c.*

*3.8. The impact of **E1** on b.c. Cell membrane permeability*

Cell membranes play a crucial role in maintaining the structural integrity of cells and ensuring normal cellular life activities. The relative

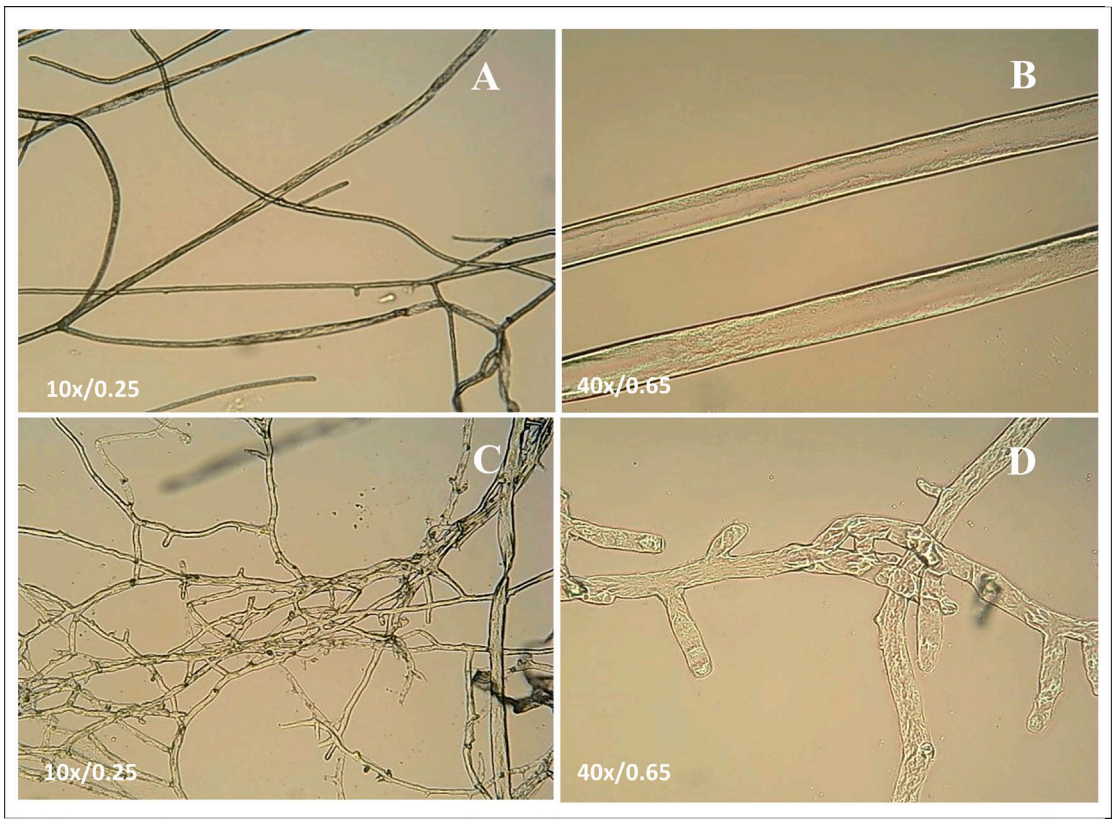

Fig. 10. The optical microscope images of *Botrytis cinerea* (*B.c.*) treated with **E1.** (A, B) 0 μg/mL and (C, D) 25 μg/mL. Scale bar for (A, C) are 10x/0.25 and Scale bar for (B, D) are 40x/0.65.

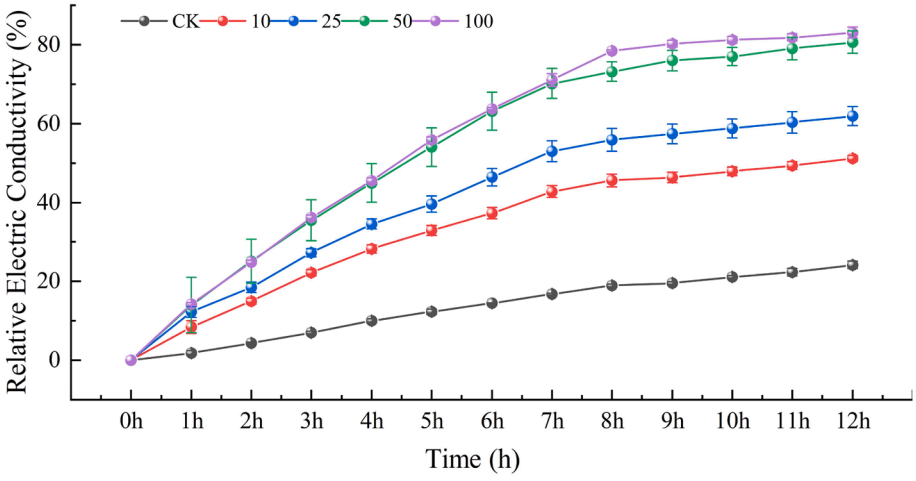

Fig. 11. Changes in cell membrane permeability of **E1** against *Botrytis cinerea* (*B.c.*).

conductivity serves as a metric to assess the permeability of these membranes. As depicted in Fig. 11, the relative conductivity of the experimental group treated with different concentrations of **E1** (0, 10, 25, 50 and 100 μg/mL) increased significantly after 12 h. When compared to the blank control group, the relative conductivity of the mycelium treated with E1 exhibited a time-dependent increase. Furthermore, as the drug concentration increased, the conductivity of the mycelium also rose, exhibiting a more pronounced upward trend compared to that of the control group. The findings revealed that **E1** had a considerable influence on the permeability of the cell membrane of *B.c.* mycelium, potentially damaging the cell membrane and causing mycelium mortality. The longer the period and the greater the concentration, the more severe the cell membrane rupture, resulting in the loss of the contents, and therefore the higher the conductivity. It increases its permeability to achieve the inhibitory action.

4. Conclusion

In this study, 21 indole derivatives containing the 1,3,4-oxadiazole moiety were designed and synthesized. These target compounds were tested for antifungal activity against 12 plant pathogenic fungi. The antifungal activity test results demonstrated that the target compounds exhibited antifungal activity against the tested plant pathogenic fungi. Among them, **E1** showed excellent antifungal activity against *B.c.*, *F.M.*,

P.s. and *S.s.* its EC_{50} values of 2.8, 5.1, 5.2 and 13.9 μg/mL were superior to those of Az, which were 15.2, 31.2, 15.2 and 18.9 μg/mL respectively. *In vivo* activity tests showed that the protective and curative effects of **E1** on blueberry leaves (91.9 % and 86.3 %) were better than Az (83.8 and 55.8 %) at the concentration of 200 μg/mL. SEM results further confirmed that **E1** could cause mycelium curling and folding, mycelium surface unevenness, and mycelium structure disruption. In addition, **E1** could change the integrity of the cell wall and cell membrane of pathogenic bacteria *B.c.*, and cause the cell membrane to rupture and the contents to leak. This resulted in enhanced malondialdehyde levels and cell membrane permeability. In conclusion, the derivatives of the 1,3,4-oxadiazole structure introduced in the indole structure had good broad-spectrum antifungal activity. The present study provides a research basis for the development of new antifungal drugs.

CRediT authorship contribution statement

Bangcan He: Performed the experiments, Analyzed the data, Writing – original draft, Writing – review & editing, Visualization. **Yuzhi Hu:** Investigation, Verify and evaluate the antifungal activity of the target compounds. **Piao Mao:** Investigation, Verify and evaluate the antifungal activity of the target compounds. **Tianyu Deng:** Investigation, Verify and evaluate the antifungal activity of the target compounds. **Yuhong Wang:** Provided the material for evaluating the antifungal activities. **Xingping Luo:** Provided the material for evaluating the antifungal activities. **Hongqian Zou:** Provided the material for evaluating the antifungal activities. **Zhenchao Wang:** Conceptualization, Design of experiments, Funding acquisition, Data supervision, Provision of experimental mapping software, Methodology. **Wei Xue:** Conceptualization, Design of experiments, Funding acquisition, Data supervision, Provision of experimental mapping software, Methodology. All authors have given approval to the final version of the manuscript.

Acknowledgements

The authors gratefully acknowledge the National Nature Science Foundation of China (22007022), the Science Foundation of Guizhou Province (No. 20192452).

Appendix A. Supplementary data

Supplementary data to this article can be found online at https://doi.org/10.1016/j.arabjc.2024.105758.

References

Alharthi, S.S., 2023. A review on indole-based colorimetric and fluorescence sensors for the detection of heavy metal ions. Chem. Pap. 77, 7379–7394.
Bräse, S., Encinas, A., Keck, J., Nising, C.F., 2009. Chemistry and biology of mycotoxins and related fungal metabolites. Chem. Rev. 109, 3903–3990.
Chen, S., Zhang, M.H., Feng, S., Gong, C.Y., Zhou, Y.X., Xing, L., He, B.C., Wu, Y.J., Xue, W., 2023. Design, synthesis and biological activity of chalcone derivatives containing pyridazine. Arab. J. Chem. 16, 104852.
Chen, Z.H., Zheng, C.J., Sun, L.P., Piao, H.R., 2010. Synthesis of new chalcone derivatives containing a rhodanine-3-acetic acid moiety with potential anti-bacterial activity. Eur. J. Med Chem. 45, 5739–5743.
Cui, Z.M., Zhou, B.H., Fu, C., Chen, L., Fu, J., Cao, F.J., Yang, X.J., Zhou, L., 2020. Simple analogues of quaternary benzo[c]phenanthridine alkaloids: discovery of a novel antifungal 2-phenylphthalazin-2-ium scaffold with excellent potency against phytopathogenic fungi. J. Agric. Food Chem. 68, 15418–15427.
Du, Q.R., Li, D.D., Pi, Y.Z., Li, J.R., Sun, J., Fang, F., Zhong, W.Q., Gong, H.B., Zhu, H.L., 2013. Novel 1,3,4-oxadiazole thioether derivatives targeting thymidylate synthase as dual anticancer/antimicrobial agents. Bioorg. Med. Chem. 21, 2286–2297.
Duan, S.F., Song, L., Guo, H.Y., Deng, H., Huang, X., Shen, Q.K., Quan, Z.S., Yin, X.M., 2023. Research status of indole-modified natural products. RSC Med. Chem. 14, 2535–2563.
Efenberger-Szmechtyk, M., Nowak, A., Czyżowska, A., Śniadowska, M., Otlewska, A., Żyżelewicz, D., 2021. Antibacterial mechanisms of aronia melanocarpa (michx.), chaenomeles superba lindl. and cornus mas L. leaf extracts. Food Chem. 350, 129218.
Fu, Y., Liu, D., Zeng, H.N., Ren, X.L., Song, B.A., Hu, D.Y., Gan, X.H., 2020. New chalcone derivatives: synthesis, antiviral activity and mechanism of action. RSC Adv. 10, 24483–24490.
Gonzalez-Fernandez, R., Jorrin-Novo, J.V., 2011. Contribution of proteomics to the study of plant pathogenic fungi. J. Proteome Res. 11, 3–16.
Hu, D., Zhang, N., Zhou, Q., Zhou, Y.X., Gong, C.Y., Zhang, Y.Q., Xue, W., 2023. Synthesis and biological activities of novel chalcone derivatives containing pyrazole oxime ethers. Fitoterapia. 166, 105458.
Ibrahim, M.K., Eissa, I.H., Abdallah, A.E., Metwaly, A.M., Radwan, M.M., ElSohly, M.A., 2017. Design, synthesis, molecular modeling and anti-hyperglycemic evaluation of novel quinoxaline derivatives as potential PPARγ and SUR agonists. Bioorg. Med. Chem. 25, 1496–1513.
Jang, J.W., Baek, J., Choi, G.D., Park, W.K., Cho, Y.S., Baek, D.J., Pae, A.N., 2012. 5-HT2C receptor selectivity and structure–activity relationship of N-methyl-N-(1-methylpiperidin-4-yl)benzenesulfonamide analogs. Bioorg. Med. Chem. Lett. 22, 347–352.
Jiang, S.C., Su, S.J., Chen, M., Peng, F., Zhou, Q., Liu, T.T., Liu, L.W., Xue, W., 2020. Antibacterial activities of novel dithiocarbamate-containing 4*H*-chromen-4-one derivatives. J. Agric. Food Chem. 68, 5641–5647.
Li, J.F., Li, D., Xu, Y.M., Guo, Z.B., Liu, X., Yang, H., Wu, L.C., Wang, L.S., 2017. Design, synthesis, biological evaluation, and molecular docking of chalcone derivatives as anti-inflammatory agents. Bioorg. Med. Chem. Lett. 27, 602–606.
Liu, F., Cao, X., Zhang, T., Xing, L., Sun, Z.L., Zeng, W., Xin, H., Xue, W., 2023. Synthesis and biological activity of myricetin derivatives containing pyrazole piperazine amide. Int. J. Mol. Sci. 24, 10442.
Liu, T.T., Peng, F., Cao, X., Liu, F., Wang, Q.F., Liu, L.W., Xue, W., 2021. Design, synthesis, antibacterial activity, antiviral activity, and mechanism of myricetin derivatives containing a quinazolinone moiety. ACS Omega. 6, 30826–30833.
Ma, D.Y., Ji, D.C., Zhang, Z.Q., Li, B.Q., Qin, G.Z., Xu, Y., Chen, T., Tian, S.P., 2019. Efficacy of rapamycin in modulating autophagic activity of *Botrytis cinerea* for controlling gray mold. Postharvest Biol. Tec. 150, 158–165.
Meşeli, T., Doğan, Ş.D., Gündüz, M.G., Kökbudak, Z., Skaro Bogojevic, S., Noonan, T., Vojnovic, S., Wolber, G., Nikodinovic-Runic, J., 2021. Design, synthesis, antibacterial activity evaluation and molecular modeling studies of new sulfonamides containing a sulfathiazole moiety. New J. Chem. 45, 8166–8177.
Nowakowska, Z., 2007. A review of anti-infective and anti-inflammatory chalcones. Eur. J. Med. Chem. 42, 125–137.
Nunes, C.A., 2011. Biological control of postharvest diseases of fruit. Eur. J. Plant Pathol. 133, 181–196.
Ouyang, Y., Li, J.J., Chen, X.Y., Fu, X.Y., Sun, S., Wu, Q., 2021. Chalcone derivatives: role in anticancer therapy. Biomolecules. 11, 894.
Peng, F., Liu, T.T., Wang, Q.F., Liu, F., Cao, X., Yang, J.S., Liu, L.W., Xie, C.W., Xue, W., 2021. Antibacterial and antiviral activities of 1,3,4-oxadiazole thioether 4*H*-chromen-4-one derivatives. J. Agric. Food Chem. 69, 11085–11094.
Peng, F., Liu, T.T., Zhu, Y.Y., Liu, F., Cao, X., Wang, Q.F., Liu, L.W., Xue, W., 2022. Novel 1,3,4-oxadiazole sulfonate/carboxylate flavonoid derivatives: synthesis and biological activity. Pest Manage. Sci. 79, 274–283.
Qian, X.H., Lee, P.W., Cao, S., 2010. China: Forward to the green pesticides via a basic research program†. J. Agric. Food Chem. 58, 2613–2623.
Ren, X.L., Li, X.Y., Yin, L.M., Jiang, D.H., Hu, D.Y., 2020. Design, synthesis, antiviral bioactivity, and mechanism of the ferulic acid ester-containing sulfonamide moiety. ACS Omega. 5, 19721–19726.
Ribas e Ribas, A.D., Spolti, P., Del Ponte, E.M., Donato, K.Z., Schrekker, H., Fuentefria, A. M., 2016. Is the emergence of fungal resistance to medical triazoles related to their use in the agroecosystems? A mini review. Braz. J. Microbiol. 47, 793-799.
Seiber, J.N., 2011. Sustainability and agricultural and food chemistry. J. Agric. Food Chem. 59, 1–21.
Shang, X.F., Zhao, Z.M., Li, J.C., Yang, G.Z., Liu, Y.Q., Dai, L.X., Zhang, Z.J., Yang, Z.G., Miao, X.L., Yang, C.J., Zhang, J.Y., 2019. Insecticidal and antifungal activities of Rheum palmatum L. anthraquinones and structurally related compounds. Ind. Crop Prod. 137, 508–520.
Silva, R.N., Monteiro, V.N., Steindorff, A.S., Gomes, E.V., Noronha, E.F., Ulhoa, C.J., 2019. Trichoderma/pathogen/plant interaction in pre-harvest food security. Fungal Biol-UK 123, 565–583.
Su, S.J., Zhou, Q., Tang, X.M., Peng, F., Liu, T.T., Liu, L.W., Xie, C.W., He, M., Xue, W., 2021. Design, synthesis, and antibacterial activity of novel myricetin derivatives containing sulfonate. Monatsh Chem. 152, 345–356.
Tang, X., Zhang, C., Chen, M., Xue, Y.N., Liu, T.T., Xue, W., 2020. Synthesis and antiviral activity of novel myricetin derivatives containing ferulic acid amide scaffolds. New J. Chem. 44, 2374–2379.
Tao, Q.Q., Liu, L.W., Wang, P.Y., Long, Q.S., Zhao, Y.L., Jin, L.H., Xu, W.M., Chen, Y., Li, Z., Yang, S., 2019. Synthesis and *in vitro* and *in vivo* biological activity evaluation and quantitative proteome profiling of oxadiazoles bearing flexible heterocyclic patterns. J. Agric. Food Chem. 67, 7626–7639.
Tleuova, A.B., Wielogorska, E., Talluri, V.S.S.L.P., Štěpánek, F., Elliott, C.T., Grigoriev, D. O., 2020. Recent advances and remaining barriers to producing novel formulations of fungicides for safe and sustainable agriculture. J. Control Release. 326, 468–481.
Wan, Z.H., Hu, D.Y., Li, P., Xie, D.D., Gan, X.H., 2015. Synthesis, antiviral bioactivity of novel 4-thioquinazoline derivatives containing chalcone moiety. Molecules. 20, 11861–11874.
Wang, Y., Yu, Y., Hou, Y.P., Mao, X.W., Liu, Z.L., Cui, J., Wang, B., Xu, S., Qian, Y.Y., Jiang, Y.Q., Wei, M., Song, P.P., 2023. Crucial role of the Ca2+/CN signaling pathway in the antifungal activity of seselin against Botrytis cinerea. J. Agric. Food Chem. 71, 9772–9781.

Wang, K.Y., Zhang, X., Shao, X.F., Wei, Y.Y., Xu, F., Wang, H.F., 2022. Flavonoids from sedum aizoon L. inhibit *Botrytis cinerea* by negatively affecting cell membrane lipid metabolism. Appl. Microbiol Biotechnol. 106, 7139–7151.

Wang, W., Zheng, X.R., Huang, X.Y., Mao, M.Z., Liu, K.Y., Xue, C., Wang, L.P., Ning, B.K., 2019. Synthesis and insecticidal evaluation of novel N-pyridylpyrazole derivatives containing diacylhydrazine/1,3,4-oxadiazole moieties. J. Heterocyclic Chem. 56, 1330–1336.

Wu, Z.J., Ouyang, M.A., Wang, C.Z., Zhang, Z.K., Shen, J.G., 2007. Anti-tobacco mosaic virus (TMV) triterpenoid saponins from the leaves of Ilex oblonga. J. Agric. Food Chem. 55, 1712–1717.

Zhang, Z.J., Jiang, Z.Y., Zhu, Q., Zhong, G.H., 2018. Discovery of β-carboline oxadiazole derivatives as fungicidal agents against rice sheath blight. J. Agric. Food Chem. 66, 9598–9607.

Zheng, S.J., Jiang, Q.J., Massande, G.N., Wu, W.B., Lin, C.S., Fang, Y., Tan, Y., Zhu, R., 2023. Synthesis and antifungal activity of indole derivatives. Chem. Nat Compd. 59, 111–118.

Zhou, Y., Gong, G.S., Cui, Y.L., Zhang, D.X., Chang, X.L., Hu, R.P., Liu, N., Sun, X.F., 2015. Identification of botryosphaeriaceae species causing kiwifruit rot in sichuan province. China. Plant Dis. 99, 699–708.

Zhou, D.G., Xie, D.D., He, F.C., Song, B.A., Hu, D.Y., 2018. Antiviral properties and interaction of novel chalcone derivatives containing a purine and benzenesulfonamide moiety. Bioorg Med Chem. Lett. 28, 2091–2097.

Zhou, R., Zhan, W.L., Yuan, C.M., Zhang, T., Mao, P., Sun, Z.L., An, Y.S., Xue, W., 2023. Design, synthesis and antifungal activity of novel 1,4-pentadiene-3-one containing quinazolinone. Int. J. Mol. Sci. 24, 2599.

Zhu, H.P., Xu, T.T., Qiu, C.Y., Wu, B.B., Zhang, Y.L., Chen, L.F., Xia, Q.Q., Li, C.L., Zhou, B., Liu, Z.G., Liang, G., 2016. Synthesis and optimization of novel allylated mono-carbonyl analogs of curcumin (MACs) act as potent anti-inflammatory agents against LPS-induced acute lung injury (ALI) in rats. Eur. J. Med. Chem. 121, 181–193.